The unusual chloroplast ATP synthase redox domain ensures enzyme activity and elevates the electrochemical proton gradient in dark-adapted *Chlamydomonas reinhardtii*.

Lando Lebok[1], Felix Buchert[1]*

[1]Institute of Plant Biology and Biotechnology, University of Münster, Münster, Germany

*Felix Buchert

Email: f.buchert@uni-muenster.de

ORCID identifier: L. L. 0000-0002-8262-1366

F. B. 0000-0001-6704-6634

Author Contributions: L. L. and F. B. performed experiments, analyzed the data, wrote and edited the manuscript. F. B. conceived, designed, and supervised the project.

FB: Conceptualization; methodology; data analysis; writing and editing manuscript, funding acquisition.

Competing Interest Statement: The authors declare no competing interests.

Classification: Plant biology, Biophysics.

Keywords: ATP synthase; Redox regulation; Photosynthesis; *Chlamydomonas reinhardtii*

Abstract

To sustain CO_2 fixation in the Calvin Benson-Bassham cycle, the multi-level regulation of the chloroplast ATP synthase (CF_1F_o) is crucial to balance the ATP output of photosynthesis with protection of the apparatus. A well-studied mechanism is thiol modulation which involves reversible cleavage of a disulfide in the γ-subunit of CF_1F_o. The disulfide in the dark-adapted enzyme from land plants establishes an inactive CF_1F_o since it requires a too high transmembrane electrochemical proton gradient ($\Delta\tilde{\mu}_{H^+}$) to catalyze ATP synthesis and hydrolysis. Here, we show in the green alga *Chlamydomonas reinhardtii* that CF_1F_o is differently regulated. Our in vivo investigation monitors the electrochromic shift (ECS) of pigments and reveals that an unusual hairpin structure in the γ-subunit redox domain lowers the algal activation threshold in CF_1F_o by ~1.4 ECS units. Thereby, thiol modulation is short-circuited so that the algal enzyme remains active in darkness. Prevention of γ-disulfide formation in a redox cysteine mutant increased the dark activity slightly which had a mild effect on raising the $\Delta\tilde{\mu}_{H^+}$ in darkness. Compared to wild type, the enzymatic activity was diminished ~3-fold in cells which carry a plant-like CF_1F_o. These mutants sustained a $\Delta\tilde{\mu}_{H^+}$ that was ~2.6 ECS units lower in the dark. Our findings point to a diversity in the regulatory integration of CF_1F_o for photosynthesis in Viridiplantae.

Introduction

The chloroplast ATP synthase (CF_1F_o) is the major H^+ gate of the photosynthetic machinery (reviewed in 1, 2). Its driving force is the transmembrane electrochemical proton gradient ($\Delta\tilde{\mu}_{H^+}$) that stems from coupled photosynthetic electron transfer and H^+ movements across the thylakoid membrane. Therefore, $\Delta\tilde{\mu}_{H^+}$ consists of a membrane potential (ΔΨ) and an osmotic component (ΔpH) which both catalyze ATP synthesis (3-6). CF_1F_o consists of two moieties, a soluble one (F_1 with subunits $\alpha_3\beta_3\gamma_1\delta_1\varepsilon_1$) and a transmembrane moiety (F_o with subunits $IV_1I_1II_1III_{14}$ or $a_1b_1b'_1c_{14}$), and the cryogenic electron microscopy structure from spinach was recently solved (7, 8). The electrochemical motor F_o translocates H^+ across the membrane through reversible protonations that drive the rotation of the c_{14}-ring. Nucleotide (de)phosphorylation takes place in the chemical motor F_1 since it contains three catalytic binding pockets within the β-subunits. Each binding site undergoes conformational switches between the empty, loose, and tight configurations (9). The switches are facilitated by the asymmetry of the rotating shaft of the γ- and ε-subunits. The two subunits are coupled to the rotating c_{14}-ring. The asymmetrical crank structure of the γ-subunit helical termini rotates within the $\alpha_3\beta_3$ barrel and forces conformational changes in the stationary β-subunit upon contact. These clashes push aside a helix-turn-helix element in the β-subunit, the DELSEED motif, thereby changing the vicinal nucleotide binding site conformation. The mechanical coupling of F_1 and F_o reactions facilitate the equilibration of the free energy stored in the phosphorylation potential [ATP]/([ADP][Pi]) and in $\Delta\tilde{\mu}_{H^+}$, respectively.

With its H^+-gating function, CF_1F_o needs to be fine-tuned for optimal photosynthetic ATP output and NADPH formation efficiency at photosystem I (PSI) to sustain CO_2 fixation in the Calvin Benson-Bassham cycle. A poor H^+ conductivity across the membrane would generate an excessive ΔpH that counters photosystem II (PSII) efficiency and stability (10, 11), eventually affecting NADPH and ATP yields. Moreover, pH-dependent nonphotochemical quenching (reviewed in 12) would become too restrictive for photochemical productivity. It has also been shown that deregulated CF_1F_o favors excessive ΔΨ spikes under fluctuating light that damage PSII (13). Therefore, CF_1F_o performance control in concert with other ion channels/antiporters (14, 15) are vital for optimal parsing of $\Delta\tilde{\mu}_{H^+}$ components. Various environmental factors regulate CF_1F_o activity such as high light, drought, or CO_2 availability (16-18) but the most well-known regulation involves "thiol modulation". A redox-active cysteine couple in the γ-subunit forms a disulfide that is cleaved enzymatically in the light (19-21) and restored in darkness (22). Disulfide cleavage lowers the $\Delta\tilde{\mu}_{H^+}$ threshold required for the onset of reversible ATP synthase activity (23,

24). Disulfide cleavage in low light allows for efficient electron flow via a highly H^+-conductive CF_1F_o. Disulfide formation was proposed to serve as an ATP-preserving strategy in the dark. However, the full scope of thiol modulation is not yet understood as mutants of the redox couple are vital in *Arabidopsis thaliana* (hereafter *A. thaliana*) (25) and *Chlamydomonas reinhardtii* (hereafter *C. reinhardtii*) (26). Nevertheless, *C. reinhardtii* ATPase is activated by a factor of ~2 when adding the thiol agent dithiothreitol to cleave the γ-disulfide in vitro (26, 27), though much higher ratios are observed in spinach enzyme in vitro (28).

We recently introduced an in vivo method that is suited for quasi-simultaneous measurements of the $\Delta\tilde{\mu}_{H^+}$ and CF_1F_o activity to examine their co-dependency during thiol modulation in *A. thaliana* (24). This method utilizes the electrochromic shift (ECS) of photosynthetic pigments because they linearly change their absorption in response to $\Delta\Psi$ (29, 30, reviewed in 31). The measurement routine is applied in dark-adapted samples where the free energy equilibrates between the phosphorylation potential [ATP]/([ADP][Pi]) and $\Delta\tilde{\mu}_{H^+}$ (i.e., $\Delta\tilde{\mu}_{H^+dark}$). Short saturating light pulses perturb the system which is monitored via exclusive changes of $\Delta\Psi$. Upon deconvolution, the measured signal amplitude provides ECS-based $\Delta\tilde{\mu}_{H^+}$ estimates and the quantified ECS decay reflects CF_1F_o activity. In this study we utilized the method to revisit thiol modulation in *C. reinhardtii* and show that it fundamentally differs from land plants.

Results

1. Dark-adapted *C. reinhardtii* displays fast ECS decay kinetics upon a laser flash and a monophasic ECS decay upon a saturating pulse

We first tried to explore whether thiol modulation is measurable in *C. reinhardtii* cells or whether it differs from land plants. A common in vivo method to visualize γ-subunit thiol modulation upon dark adaptation is the use of flash-induced ECS decay kinetics (25, 32). The assumption is to link a fast ECS decay to a highly active enzyme in the presence of a γ-dithiol. Flash-induced ECS measurements were carried out in a collection of land plants and *C. reinhardtii* (Figure 1A). All samples were dark-adapted for 30 min and, as shown in the inset, the typical three phases of the ECS kinetics were visible (reviewed in 31): The rapid ECS increase was attributed to PSI and PSII charge separation activity (a-phase, established before the first measurement after the flash). The first phase was followed by a ~10-ms rise in ECS which is related to charge separation in the low-potential chain of the cytochrome b_6f complex (b-phase). Finally, the ECS decay mainly results from ATP synthesis activity through CF_1F_o (c-phase). Clearly, the latter phase was most rapid in dark-adapted *C. reinhardtii* cells. However, we recently pointed out that the amplitude of the $\Delta\tilde{\mu}_{H^+}$ at the time of flash ECS measurements strongly influences the speed of the c-phase, which is accelerated at high $\Delta\tilde{\mu}_{H^+}$ regardless of thiol modulation (24). Thus, at high $\Delta\tilde{\mu}_{H^+}$ both CF_1F_o states are equally active in vivo which is in line with original in vitro reports on the $\Delta\tilde{\mu}_{H^+}$ dependency of thiol-modulated CF_1F_o (23). The flash results are therefore only a hint but not suitable for concluding on the presence or absence of thiol modulation in *C. reinhardtii*.

We then used the pulse ECS method to search for a slowdown in the decay after ~100 ms darkness which we linked to the formation of a γ-disulfide in *A. thaliana* (24). With this method the thylakoid membranes are maximally energized during multiple turnovers until a plateau in the ECS rise is observed after several ms of saturating light. The ECS decay during the following dark period reflects mainly ATP synthesis and can last several seconds until reaching the pre-pulse equilibrium. After the fast initial decay phase the kinetics showed a typical slowdown in dark-adapted *A. thaliana* leaves (Figure 1B). This slowdown occurred between 50 ms and 100 ms of darkness when ~60% of the ECS decayed back to the pre-pulse level. Contrary, the decay was monophasic in *C. reinhardtii*. Within ~1 s of darkness the pulse-induced ECS signals decayed to the level before the measurement. For better comparison we chose to show relative units, setting

the ECS plateau to 1 since the ECS probe density per photosystem reaction centers likely varies across species. In the next sections we mutated several residues in the *C. reinhardtii* γ-subunit to further examine the origin of the monophasic ECS decay.

2. The mutation of the γ-disulfide enhances the ECS decay and rises the $\Delta\tilde{\mu}_{H^+dark}$.

To test whether absence of the γ-disulfide upon mutation had an impact on the ECS kinetics, we mutated *C. reinhardtii* γC233S which corresponds to the CF_1F_o γ-cysteine at position 199 in the mature spinach polypeptide. Figure 2A shows that the flash ECS kinetics were further accelerated in the dark-adapted mutant. This suggests that the wild type activity was partially restricted in the dark. The c-phase in the mutant was so rapid that no apparent b-phase was detectable. Figure 2B demonstrates that the pulse-induced ECS amplitude was smaller upon disrupting the cysteine couple. Here the ECS units were expressed in PSI charge separations (see Materials and Methods). The ECS plateau shortly before t = 0 ms reflects a threshold upon which no further membrane energization is obtained (24, 33). The saturating pulse duration had to be extended in γC233S to reach this threshold, still it was below 100 ms where ΔpH started to form (24). Although the initial slopes of the rising ECS were comparable, the *smaller* ECS signal amplitude during the pulse in the mutant indicates that the $\Delta\tilde{\mu}_{H^+dark}$ before the measurement was *higher*. Apart from the higher $\Delta\tilde{\mu}_{H^+dark}$ before and after this γC233S measurement, the ECS decay was very similar directly after switching off the pulse (Figure 2B) and monophasic (Figure 2C). The pre-pulse ECS level was reached within less than 1 s in both samples. In the next section we focus on the primary structure of the algal γ-subunit redox domain and simulated thiol modulation as it is known from vascular plants.

3. The amino acid sequence of the second hairpin in the γ-subunit determines the $\Delta\tilde{\mu}_{H^+dark}$.

The original CF_1F_o structure from spinach revealed several interactions between the rotor and stator subunits (7). One of them is a salt bridge which is formed between γ-glutamate 220 within the second hairpin of the redox domain and β-arginine 397 in the DELSEED loop (Figure 3A). The amino acids of this γ-subunit hairpin are rather conserved among land plants and mosses (Figure 3B). Interestingly, the *C. reinhardtii* sequence stands out since the negative glutamate (arrowhead in Figure 3B) is replaced by a glycine and shifted to a position that is occupied by a positively charged residue in land plants. Moreover, an alanine is found instead of a serine/threonine in close vicinity. Note that the selected plant sequences are from the samples examined in Figure 1A and in literature (33), respectively. Based on those differences we decided to swap the γ-segment ^{254}GGEFE^{258} (*C. reinhardtii* numbering including ATPC transit peptide) with the *A. thaliana* fragment EGKLT (underlined in Figure 3B). This *C. reinhardtii* mutant, dubbed γAt-loop, showed plant-like ECS kinetics upon a laser flash (Figure 3C, cf. diamond and triangle symbols, and plants in Figure 1A). When acknowledging the difference in basal membrane energization until reaching the same maximum at the end of the pulse (see Materials and Methods), the $\Delta\tilde{\mu}_{H^+dark}$ was ~2 PSI charge separations lower in the mutant compared to wild type (Figure 3D). After the pulse, the ECS decay in the dark displayed two phases in γAt-loop: a rapid one finished in ~100 ms was followed by a slower phase (Figure 3E). In this regard, the ECS decay after a pulse was similar in dark-adapted γAt-loop and vascular plants (24, 33). The ECS signals returned to the pre-pulse level within ~20 s darkness. The circle symbols of panels C-E in Figure 3 also shows γAt-loop/γC233S; a plant-like variant which is unable to form a disulfide. The ECS decay both upon ns flash (Figure 3C) and ms pulse (Figure 3E) were accelerated in the double mutant which also showed a higher $\Delta\tilde{\mu}_{H^+dark}$ compared to γAt-loop as well as wild type (Figure 3D). Judging from the raw ECS kinetics, the prevention of a γ-disulfide formation via γC233S had similar effects in the algal loop background (Figure 2) and the plant like γAt-loop (Figure 3C-3E).

The advantage of the ECS pulse method is to plot CF_1F_o activity vs. $\Delta\tilde{\mu}_{H^+dark}$ in vivo (24), which is what we did in Figure 4 in a slightly modified form (see Materials and Methods). The stromal [ATP]/([ADP][Pi]) concentration ratio is in equilibrium with the $\Delta\tilde{\mu}_{H^+dark}$, and after inducing a short perturbation via the light pulse the samples returned, mainly via ATP synthesis, to that state within at least ~30 s darkness. Accordingly, CF_1F_o activity in disequilibrated samples could be measured at distinct $\Delta\tilde{\mu}_{H^+}$. Figure 4A shows independent biological replicates of the four *C. reinhardtii* strains which displayed some $\Delta\tilde{\mu}_{H^+dark}$ variation. While only an insignificant increase in $\Delta\tilde{\mu}_{H^+dark}$ was seen in both γC233S variants, a clear decrease to -8.9 ± 0.4 PSI charge separations was obtained in γAt-loop (opposed to -6.3 ± 0.6 in wild type). We quantified the ECS-based CF_1F_o activities from pulse-induced decay kinetics showed earlier. The wild type activities in Figure 4B ranged from 0 at the $\Delta\tilde{\mu}_{H^+dark}$ level on the very left (when activities of ATP synthesis and hydrolysis were equal) to ~45 PSI charge separations s^{-1} at $\Delta\tilde{\mu}_{H^+dark}$ + 5 units. Measurable wild type CF_1F_o activities of ~6 PSI charge separations s^{-1} were detected at $\Delta\tilde{\mu}_{H^+dark}$ + 2 units, i.e., at a $\Delta\tilde{\mu}_{H^+}$ of -4.3 ± 0.6 PSI charge separations. The γAt-loop showed this activity onset much higher at $\Delta\tilde{\mu}_{H^+}$ of -2.9 ± 0.4 units. This points to a higher energy stored as $\Delta\tilde{\mu}_{H^+}$ that is required to activate the γAt-loop in the dark-adapted state. Moreover, an extrapolation of the wild type data yielded a ~3-fold more active CF_1F_o at $\Delta\tilde{\mu}_{H^+}$ of -3 units. When abolishing thiol modulation via γC233S in Figure 4C, no significant differences were observed compared to wild type. Figure 4D shows that the detected inactivity of dark-adapted γAt-loop was recovered by an additional γC233S.

Discussion

It has long been established that microalgae sustain a substantial $\Delta\tilde{\mu}_{H^+dark}$ via a CF_1F_o-dependent mechanism (34-36). Besides its detection, the authors could define the $\Delta\tilde{\mu}_{H^+}$ partitioning into ΔΨ and ΔpH, and that it is altered in metabolic conditions. Their data suggests that the $\Delta\tilde{\mu}_{H^+dark}$ ranges from 20-50 mV (34) and was around ~1.5 ΔpH units (35) especially upon anaerobiosis. In the absence of CF_1F_o the ΔpH was absent in the mutants and $\Delta\tilde{\mu}_{H^+dark}$ was dominated by ΔΨ (36).

Our study was inspired from the unusual pulse-induced ECS kinetics of dark-adapted *C. reinhardtii*. The short pulse drives ATP synthesis for several seconds until reaching an equilibrium close to the situation right before the measurements. Transitioning to darkness with a maximally energized membrane at the end of the pulse, the ECS decay slowdown is due to an energetic activation threshold that the system is falling below after synthesizing ATP for ~100 ms. When reaching $\Delta\tilde{\mu}_{H^+dark}$ at a much lower level the ECS decay finishes and a match in free energy stored in the [ATP]/([ADP][Pi]) concentration ratio is established. Absence of an ECS slowdown in *A. thaliana* under γ-dithiol favoring conditions is due to threshold tuning of this activation barrier to a lower value (24). As a result, the multiphasic ECS decay changed to a monophasic one in *A. thaliana*.

Based on the monophasic pulse kinetics that we introduced in Figure 1B, one could assume that (i) the γ-disulfide is absent in dark-adapted *C. reinhardtii*. (ii) Alternatively, the kinetics could also result from increased ATP levels so that the free energy in the [ATP]/([ADP][Pi]) concentration ratio in the dark is shifted to higher values, thus favoring ATP hydrolysis and a substantial increase of $\Delta\tilde{\mu}_{H^+dark}$. This way the energetic activation barrier of algal CF_1F_o could be surpassed despite a γ-disulfide, as has been shown in *A. thaliana* leaves (24). (iii) It could also be that the $\Delta\tilde{\mu}_{H^+}$ activation threshold in algal CF_1F_o is exceptionally low due to other structural features that escape or tolerate limitations imposed by a γ-disulfide in darkness as we know from plants.

A first hint that the γ-disulfide is indeed present in *C. reinhardtii* is presented in Figure 2 where a higher $\Delta\tilde{\mu}_{H^+dark}$ was sustained in γC233S. This shows that the stored energy in the

[ATP]/([ADP][Pi]) ratio under physiological conditions is not exhausted in wild type and can be more efficiently converted to $\Delta\tilde{\mu}_{H^+dark}$ by γC233S. These finding are against (i) and (ii). Instead, in Figures 3 and 4 we provide evidence in favor of (iii). The strongly repressed γAt-loop that shows an ECS slowdown with a plant-like hairpin is not able to stay active despite a hypothetically high [ATP]/([ADP][Pi]) ratio, ruling out (ii). The mutant is fully restored via γC233S only, ruling out (i).

Instead, the rotating hairpin segment in *C. reinhardtii* may not be as prone to form salt bridges with the β-DELSEED loop as in land plants. This could influence the DELSEED motion upon clashes with the rotor and thus alter the (un)binding of ATP, ADP and Pi. Accordingly, a change in chemical-to-mechanical energy transduction in CF_1 may lower the energetic activation barrier of the enzyme in the presence of a γ-disulfide. Indeed, the quantified activity onset of wild type CF_1F_o in Figure 4B (~-4.3 $\Delta\tilde{\mu}_{H^+}$ units) was below that of wild type *A. thaliana* at ~-2.2 $\Delta\tilde{\mu}_{H^+}$ units (24). Interestingly, the $\Delta\tilde{\mu}_{H^+}$ activation in γAt-loop was closer to the one in *A. thaliana* (~-2.9 $\Delta\tilde{\mu}_{H^+}$ units, Figure 4B). Assuming that (ii) is ruled out, the standard free energy change of ATP synthesis/hydrolysis is increased in the wild type alga. Thus, the *C. reinhardtii* CF_1F_o manages to convert the free energy stored in the existing [ATP]/([ADP][Pi]) concentration ratio to match with a higher $\Delta\tilde{\mu}_{H^+dark}$ compared to land plants.

This raises the question why *C. reinhardtii* operates at an elevated chloroplast $\Delta\tilde{\mu}_{H^+dark}$. Clearly, the $\Delta\tilde{\mu}_{H^+}$ has many regulatory functions and such an investment could pay off eventually – possibly due to a unique *C. reinhardtii* feature combination. For instance, the CO_2 concentrating mechanism in aquatic phototrophs is believed to require an acidified lumen for carbonic anhydrase 3 to dehydrate HCO_3^- (37, 38), and the algal CF_1F_o may facilitate a primed system by its capacity of hydrolyzing ATP more efficiently. The lumen pH is also important for photoprotection. Nonphotochemical quenching is not always expressed in *C. reinhardtii* as LHCSR3 expression is tightly controlled (39, 40). Constitutive in land plants, in *C. reinhardtii* the ΔpH-dependent photoprotection response through controlled PSII de-excitation may not always take place. An acidic lumen also triggers the "photosynthetic control" process to protectively restrict electron flow via the cytochrome b_6f complex (41-43). It is known that the deposition of H^+ into the lumen upon plastoquinol oxidation is less favorable at excessive ΔpH. Since the algal H^+ conductivity via CF_1F_o remains high in the dark, an onset of photosynthetic control during the light induction period should be more unlikely. *C. reinhardtii* may tolerate the active CF_1F_o that does not underly light-dependent thiol modulation because of unique PSI electron sinks such as flavodiiron proteins. These have been shown to play a role during the induction of photosynthesis (44). Interestingly, photosynthetic control was routinely inducible in *A. thaliana* when measuring a lumen pH-sensitive cytochrome b_6f complex mutant under moderate light conditions (45). To cause an electron flow limitation in the cytochrome b_6f complex, the homologous mutant in *C. reinhardtii* required additional environmental cues that slow down CF_1F_o, among other responses (46). By escaping thiol modulation the algal CF_1F_o may play a role in this species-specific ΔpH feedback on the mutated cytochrome b_6f complex.

Taken together, this study shows that thiol modulation still holds some secrets despite being one of the most investigated CF_1F_o regulation mechanisms. Since *C. reinhardtii* wild type (and γC233S) is viable with an active ATPase in the dark, this redox switch did most likely not evolve in the green lineage to conserve ATP at night. It is possible that individual features of a photosynthetic eukaryote may require a differently weighted integration of thiol modulation within the overall CF_1F_o regulation network. Evidently, more research is needed to explore the versatility of photosynthesis regulation in the presence and absence of the redox switch.

Materials and Methods

Transformation and growth of *Chlamydomonas reinhardtii* strains

The transformation plasmid was published previously (16) and is based on the pPEARL expression vector (GenBank: KU531882.1). The *ATPC* CDS was cloned as a *Bam*HI/*Eco*RI fragment using ATPC.F forward (5'GTTCGAATTCATGGCCGCTATGCTCGCC) and reverse ATPC.R primers (5'GCCAGGATCCTTAGCCCGAGGTGGCGGCG). The hairpin that encodes the amino acids ^{254}GGEFE^{258} (*C. reinhardtii* numbering including ATPC transit peptide) was mutated using abutting primers hp.F (5'CAAGCTGACCGTGGAGCGCGAGAAGACC) and hp.R (5'CCCTCCTTGGTGGTCAGCTTGAAGATCTC), indicating underscored mismatches. The 323-bp PCR fragments of ATPC.R/hp2.F and the 775-bp fragment of ATPC.F/hp2.R were ligated, followed by another round of PCR using primers ATPC.F/ATPC.R. The redox-active cysteine couple was disrupted by mutating one of the cysteines at position 233 to serine, using the CS.F (5'CCCATGGGCGAGCTGTCGGACGTGGACGGCAAG). The 406-bp PCR fragment of CS.F/ATPC.R was used in a megaprimer approach (47) to yield the mutated *ATPC* gene in combination with oligos ATPC.F/ATPC.R.

The recipient strain for nuclear transformation did not accumulate *ATPC* transcripts (48) and was cultured on acetate-supplemented TAP medium (49) due to lack of phototropic growth. Transformants were obtained by electroporation (50) using 25 µF and 1000 V cm^{-1}. All successful transformants displayed phototrophic growth and were cultured under diurnal 16-h photoperiods of 50 µmol photons m^{-2} s^{-1} at 23°C on agar-supplemented and liquid Tris-minimal medium in the absence of acetate (49). Liquid cultures were bubbled with sterile air and kept in the exponential phase (0.5–3 $\times$ 10^6 cells/mL) at 23°C by regular dilutions. Air bubbling ensured CO_2 supply for the Calvin-Benson-Bassham cycle. The experiments in Figure 1 show the t222+ wild type strain.

Cultivation of land plants

The *Arabidopsis thaliana* (Columbia ecotype) and *Pisum sativum* var. *arvense* were cultivated on soil at 23°C under diurnal 16-h photoperiods of 150 µmol photons m^{-2} s^{-1}. *Physcomitrium patens* Gransden wild type was grown at 23°C on $PpNO_3$ minimum medium (51) under diurnal 16-h photoperiods of 80 µmol photons m^{-2} s^{-1}. Leaves from *Ginkgo biloba*, *Sorghum bicolor*, and *Triticum aestivum* were obtained from the Botanical Garden of the University of Münster on August 1, 2018 (cloudy, 24°C).

In vivo spectroscopy

The electrochromic shift (ECS) of photosynthetic pigments was used as an in vivo tool to study the linear relationship of ECS signals with $\Delta\Psi$, the electric $\Delta\tilde{\mu}_{H^+}$ component (29, 30, reviewed in 31). The ECS was measured as the ΔI/I difference at wavelengths 520 nm – 546 nm in a Joliot-type spectrophotometer (JTS-10, Biologic, France). White pulsed LED detection light was passed through respective interference filters (FWHM: 20 nm). The light-detecting diodes were protected from scattered actinic light by 3-mm BG39 filters (Schott, Mainz, Germany). Illumination of the samples was interrupted by short dark intervals (250 µs) during which 10-µs detecting pulses were placed after 200 µs. An ECS assay for dark-adapted samples uses short saturating light pulses with a duration of several ms to estimate the $\Delta\tilde{\mu}_{H^+}$ levels in leaves of *Spinacia oleracea* (33) and *Arabidopsis thaliana* (24), which will be used here. This method uses as experimental reference the ECS value after the short light pulse at 10 ms darkness, which is set to 0. This is necessary because the absolute value of the ECS-based $\Delta\tilde{\mu}_{H^+dark}$ is unknown and instead it is expressed in negative values below the experimental reference 0 (cf. Ref. 24 and Supplemental Materials and Methods for further details).

The ECS protocol also involves a dark period after the pulse which is used to quantify ATP synthesis activity. The ECS decay is reflecting mainly CF_1F_o-related processes and the kinetics are quantified at defined units above the measured $\Delta\tilde{\mu}_{H^+dark}$ (24). Here we used several single-

exponential fitting functions on one ECS decay curve with a series of amplitudes (between 1 and 6 units) which was multiplied with the respective rate constant to obtain the CF_1F_o activity.

All algal absorption changes were normalized to the ECS $\Delta I/I$ signals produced after a saturating 6-ns laser flash in the presence of 1 mM hydroxylamine and 10 µM 3-(3,4-dichlorophenyl)-1,1-dimethylurea, which relate to the density of active PSI centers in the sample. Thus, the unit of 1 PSI charge separation is produced when measuring the flash-induced ECS amplitude (rapidly established before the first detection at ~300-µs). Accordingly, the ECS-based CF_1F_o activity is expressed in PSI charge separations s^{-1}. For land plants, it was assumed that both photosystems were equally abundant and a multiplication of the kinetics by 0.5 times the rapid ECS amplitude yielded signals expressed as PSI charge separation units. All shown kinetics were obtained in the presence of PSII activity.

Acknowledgments

This work was supported by a grant from the Deutsche Forschungsgemeinschaft (BU 3426/3-1). We would like to thank Prof. Michael Hippler for stimulating discussions.

References

1. F. Buchert, "Chapter Three - Chloroplast ATP synthase from green microalgae" in Advances in Botanical Research, T. Hisabori, Ed. (Academic Press, 2020), vol. 96, pp. 75-118.
2. W. Junge, N. Nelson, ATP synthase. *Annu. Rev. Biochem.* **84**, 631-657 (2015).
3. J. H. Kaplan, E. Uribe, A. T. Jagendorf, ATP hydrolysis caused by acid-base transition of spinach chloroplasts. *Arch Biochem Biophys* **120**, 365-370 (1967).
4. P. Gräber, H. T. Witt, Relations between the electrical potential, pH gradient, proton flux and phosphorylation in the photosynthetic membrane. *Biochim. Biophys. Acta* **423**, 141-163 (1976).
5. D. A. Harris, A. R. Crofts, The initial stages of photophosphorylation. Studies using excitation by saturating, short flashes of light. *Biochim. Biophys. Acta* **502**, 87-102 (1978).
6. D. M. Kramer, A. R. Crofts, Activation of the chloroplast ATPase measured by the electrochromic change in leaves of intact plants. *Biochimica et Biophysica Acta* **976**, 28-41 (1989).
7. A. Hahn, J. Vonck, D. J. Mills, T. Meier, W. Kuhlbrandt, Structure, mechanism, and regulation of the chloroplast ATP synthase. *Science* **360** (2018).
8. J. H. Yang, D. Williams, E. Kandiah, P. Fromme, P. L. Chiu, Structural basis of redox modulation on chloroplast ATP synthase. *Communications biology* **3**, 482 (2020).
9. P. D. Boyer, The binding change mechanism for ATP synthase - some probabilities and possibilities. *Biochim. Biophys. Acta* **1140**, 215-250 (1993).
10. A. Krieger, E. Weis, The role of calcium in the pH-dependent control of Photosystem II. *Photosynth Res* **37**, 117-130 (1993).
11. I. Zaharieva, J. M. Wichmann, H. Dau, Thermodynamic limitations of photosynthetic water oxidation at high proton concentrations. *J. Biol. Chem.* **286**, 18222-18228 (2011).
12. K. K. Niyogi, T. B. Truong, Evolution of flexible non-photochemical quenching mechanisms that regulate light harvesting in oxygenic photosynthesis. *Curr. Opin. Plant Biol.* **16**, 307-314 (2013).
13. G. A. Davis *et al.*, Limitations to photosynthesis by proton motive force-induced photosystem II photodamage. *Elife* **5** (2016).

14. U. Armbruster *et al.*, Ion antiport accelerates photosynthetic acclimation in fluctuating light environments. *Nat Commun* **5**, 5439 (2014).
15. A. Herdean *et al.*, A voltage-dependent chloride channel fine-tunes photosynthesis in plants. *Nat Commun* **7**, 11654 (2016).
16. F. Buchert, B. Bailleul, T. Hisabori, A γ-subunit point mutation in *Chlamydomonas reinhardtii* chloroplast F_1F_o-ATP synthase confers tolerance to reactive oxygen species. *Biochim. Biophys. Acta* **1858**, 966-974 (2017).
17. K. Kohzuma *et al.*, The long-term responses of the photosynthetic proton circuit to drought. *Plant Cell Environ.* **32**, 209-219 (2009).
18. A. Kanazawa, D. M. Kramer, *In vivo* modulation of nonphotochemical exciton quenching (NPQ) by regulation of the chloroplast ATP synthase. *Proc. Natl. Acad. Sci. USA* **99**, 12789-12794 (2002).
19. B. Naranjo *et al.*, The chloroplast NADPH thioredoxin reductase C, NTRC, controls non-photochemical quenching of light energy and photosynthetic electron transport in Arabidopsis. *Plant Cell Environ* **39**, 804-822 (2016).
20. J. D. Mills, P. Mitchell, P. Schurmann, Modulation of coupling factor ATPase activity in intact chloroplasts - The role of the thioredoxin system. *FEBS Lett.* **112**, 173-177 (1980).
21. L. R. Carrillo, J. E. Froehlich, J. A. Cruz, L. J. Savage, D. M. Kramer, Multi-level regulation of the chloroplast ATP synthase: the chloroplast NADPH thioredoxin reductase C (NTRC) is required for redox modulation specifically under low irradiance. *Plant J.* **87**, 654-663 (2016).
22. K. Yoshida, A. Hara, K. Sugiura, Y. Fukaya, T. Hisabori, Thioredoxin-like2/2-Cys peroxiredoxin redox cascade supports oxidative thiol modulation in chloroplasts. *Proc. Natl. Acad. Sci. USA* **115**, E8296-E8304 (2018).
23. U. Junesch, P. Gräber, Influence of the redox state and the activation of the chloroplast ATP synthase on proton-transport-coupled ATP synthesis hydrolysis. *Biochim. Biophys. Acta* **893**, 275-288 (1987).
24. F. Buchert, B. Bailleul, P. Joliot, Disentangling chloroplast ATP synthase regulation by proton motive force and thiol modulation in Arabidopsis leaves. *Biochim. Biophys. Acta* **1862**, 148434 (2021).
25. G. Wu, D. R. Ort, Mutation in the cysteine bridge domain of the γ subunit affects light regulation of the ATP synthase but not photosynthesis or growth in Arabidopsis. *Photosynthesis Res.* **97**, 185-193 (2008).
26. S. A. Ross, M. X. Zhang, B. R. Selman, Role of the *Chlamydomonas reinhardtii* coupling factor-1 γ subunit cysteine bridge in the regulation of ATP synthase. *J. Biol. Chem.* **270**, 9813-9818 (1995).
27. D. Hu, H. Strotmann, N. Shavit, S. Leu, The *C. reinhardtii* CF_1 with the mutation βT168S has high ATPase activity. *FEBS Lett.* **421**, 65-68 (1998).
28. R. E. McCarty, E. Racker, Partial resolution of the enzymes catalyzing photophosphorylation. 3. Activation of adenosine triphosphatase and ^{32}P-labeled orthophosphate-adenosine triphosphate exchange in chloroplasts. *J. Biol. Chem.* **243**, 129-137 (1968).
29. W. Junge, H. T. Witt, On the ion transport system of photosynthesis--investigations on a molecular level. *Z Naturforsch B* **23**, 244-254 (1968).
30. H. T. Witt, Energy conversion in the functional membrane of photosynthesis. Analysis by light pulse and electric pulse methods. The central role of the electric field. *Biochim. Biophys. Acta* **505**, 355-427 (1979).
31. B. Bailleul, P. Cardol, C. Breyton, G. Finazzi, Electrochromism: a useful probe to study algal photosynthesis. *Photosynthesis Res.* **106**, 179-189 (2010).
32. K. Kohzuma *et al.*, Thioredoxin-insensitive plastid ATP synthase that performs moonlighting functions. *Proc. Natl. Acad. Sci. USA* **109**, 3293-3298 (2012).
33. P. Joliot, A. Joliot, Quantification of the electrochemical proton gradient and activation of ATP synthase in leaves. *Biochim. Biophys. Acta* **1777**, 676-683 (2008).

34. P. Joliot, A. Joliot, Characterization of linear and quadratic electrochromic probes in *Chlorella sorokiniana* and *Chlamydomonas reinhardtii*. *Biochim. Biophys. Acta* **975**, 355-360 (1989).
35. G. Finazzi, F. Rappaport, *In vivo* characterization of the electrochemical proton gradient generated in darkness in green algae and its kinetic effects on cytochrome b_6f turnover. *Biochemistry* **37**, 9999-10005 (1998).
36. F. Rappaport, G. Finazzi, Y. Pierre, P. Bennoun, A new electrochemical gradient generator in thylakoid membranes of green algae. *Biochemistry* **38**, 2040-2047 (1999).
37. J. V. Moroney, R. A. Ynalvez, Proposed carbon dioxide concentrating mechanism in Chlamydomonas reinhardtii. *Eukaryot. Cell* **6**, 1251-1259 (2007).
38. M. H. Spalding, Microalgal carbon-dioxide-concentrating mechanisms: Chlamydomonas inorganic carbon transporters. *J. Exp. Bot.* **59**, 1463-1473 (2008).
39. G. Peers *et al.*, An ancient light-harvesting protein is critical for the regulation of algal photosynthesis. *Nature* **462**, 518-521 (2009).
40. G. Allorent *et al.*, UV-B photoreceptor-mediated protection of the photosynthetic machinery in Chlamydomonas reinhardtii. *Proc Natl Acad Sci U S A* **113**, 14864-14869 (2016).
41. B. Rumberg, U. Siggel, pH changes in the inner phase of the thylakoids during photosynthesis. *Naturwissenschaften* **56**, 130-132 (1969).
42. A. N. Tikhonov, G. B. Khomutov, E. K. Ruuge, L. A. Blumenfeld, Electron transport control in chloroplasts. Effects of photosynthetic control monitored by the intrathylakoid pH. *Biochimica et Biophysica Acta (BBA) - Bioenergetics* **637**, 321-333 (1981).
43. J. N. Nishio, J. Whitmarsh, Dissipation of the Proton Electrochemical Potential in Intact Chloroplasts (II. The pH Gradient Monitored by Cytochrome f Reduction Kinetics). *Plant Physiol.* **101**, 89-96 (1993).
44. F. Chaux *et al.*, Flavodiiron Proteins Promote Fast and Transient O_2 Photoreduction in Chlamydomonas. *Plant Physiol.* **174**, 1825-1836 (2017).
45. Y. Munekage *et al.*, Cytochrome b(6)f mutation specifically affects thermal dissipation of absorbed light energy in Arabidopsis. *Plant J.* **28**, 351-359 (2001).
46. S.-I. Ozawa, F. Buchert, R. Reuys, M. Hippler, Y. Takahashi, The algal PETC-Pro171-Leu suppresses electron transfer in the cytochrome b_6f complex under acidic lumenal condition. *bioRxiv* 10.1101/2021.12.15.472847, 2021.2012.2015.472847 (2022).
47. O. Landt, H. P. Grunert, U. Hahn, A general method for rapid site-directed mutagenesis using the polymerase chain reaction. *Gene* **96**, 125-128 (1990).
48. D. Drapier, B. Rimbault, O. Vallon, F. A. Wollman, Y. Choquet, Intertwined translational regulations set uneven stoichiometry of chloroplast ATP synthase subunits. *EMBO J.* **26**, 3581-3591 (2007).
49. D. S. Gorman, R. P. Levine, Cytochrome *f* and plastocyanin: their sequence in the photosynthetic electron transport chain of *Chlamydomonas reinhardtii*. *Proc Natl Acad Sci U S A* **54**, 1665-1669 (1965).
50. C. Raynaud *et al.*, Evidence for regulatory function of nucleus-encoded factors on mRNA stabilization and translation in the chloroplast. *Proc Natl Acad Sci U S A* **104**, 9093-9098 (2007).
51. N. W. Ashton, N. H. Grimsley, D. J. Cove, Analysis of gametophytic development in the moss, Physcomitrella patens, using auxin and cytokinin resistant mutants. *Planta* **144**, 427-435 (1979).

Figures and Tables

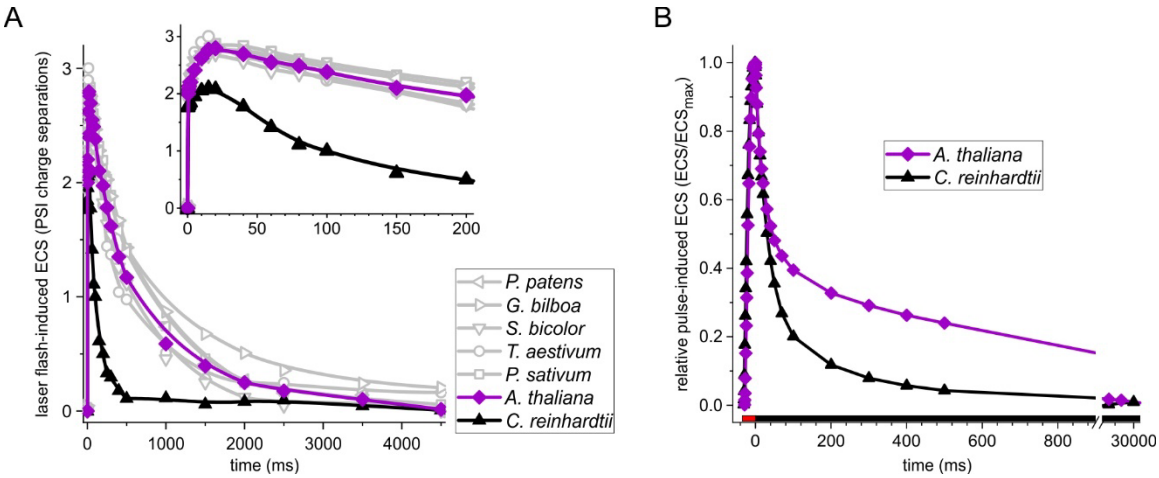

Figure 1. Measurements of the electrochromic shift (ECS) demonstrate that, unlike land plants, *C. reinhardtii* harbors an active CF_1F_o in dark-adapted samples. (A) The ECS decay upon a single-turnover laser flash reflects the de-energization of the photosynthetic membrane mainly via ATP synthesis activity. This process is markedly accelerated in the green algal sample. (B) The maximal ECS signal is reached within a few ms of a multiple-turnover saturating light pulse (red bar), and sample-specific decay phases are recorded in the dark (black bar). While *A. thaliana* ECS decay slows down after ~100 ms darkness, the process is monophasic in dark-adapted *C. reinhardtii*. The other plants shown in Figure 1 are *Physcomitrium patens, Ginkgo biloba*, *Sorghum bicolor*, *Triticum aestivum* and *Pisum sativum*.

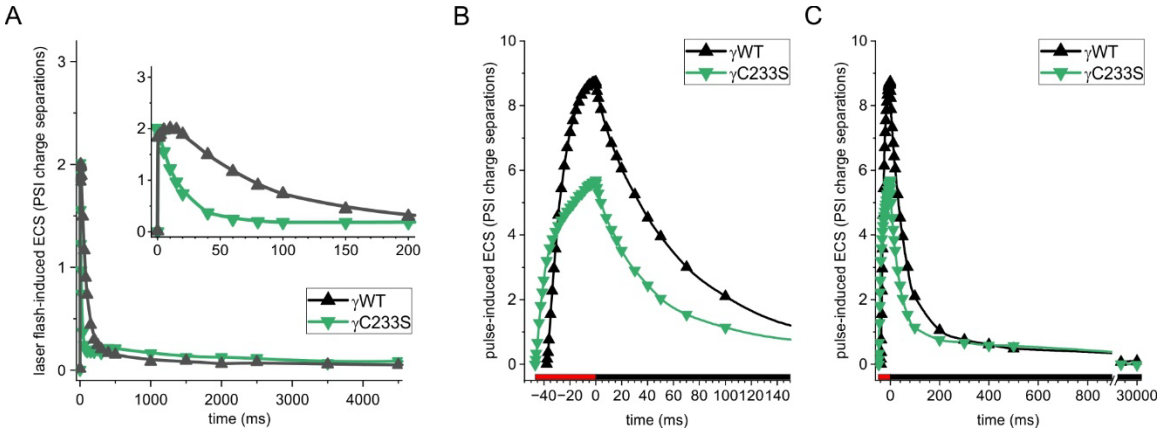

Figure 2. Measurements of the electrochromic shift (ECS) in dark-adapted samples demonstrate that *C. reinhardtii* CF_1F_o activity in vivo is further amplified upon abolishing thiol modulation. (A) The ECS decay was accelerated in γC233S as it does not form a γ-disulfide. (B) The ECS amplitude during a saturating light pulse is smaller in γC233S due to a higher $\Delta\tilde{\mu}_{H^+dark}$ (see Materials and Methods). The initial buildup and decay of the pulse-induced ECS resembles the wild type. (C) The overall signal decay is also similar in both samples, showing monophasic kinetics.

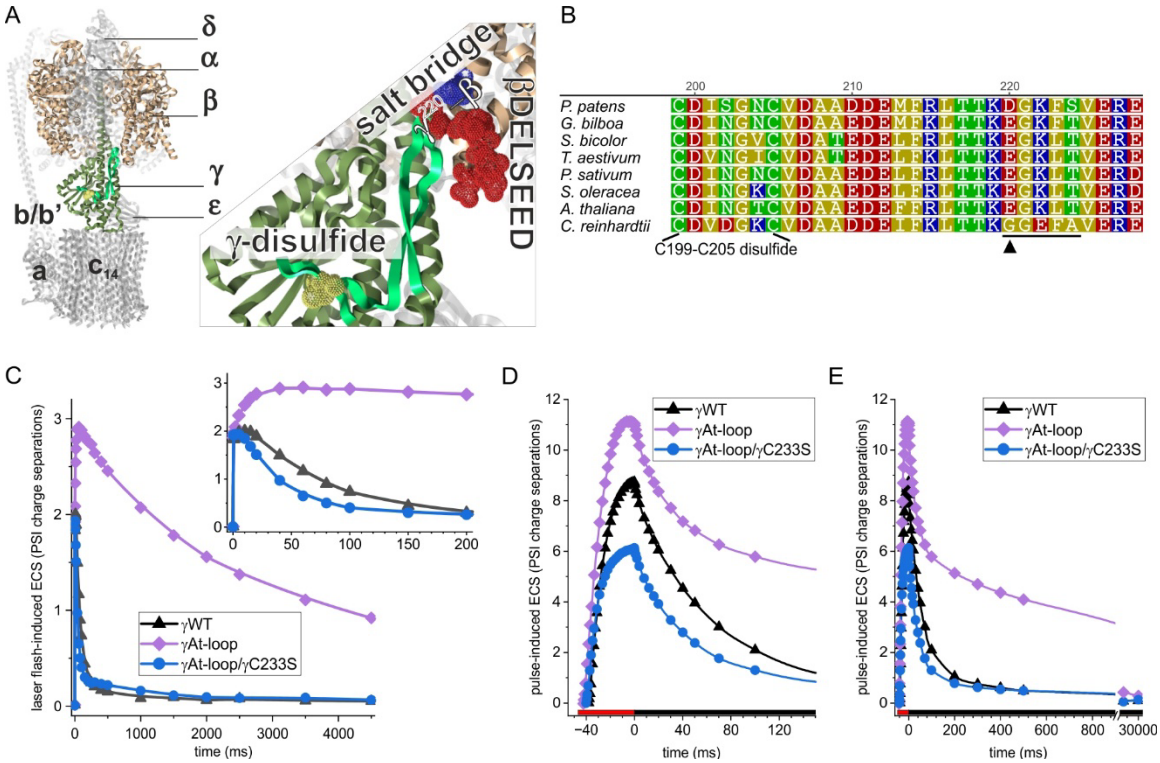

Figure 3. Structural comparison and measurements of the electrochromic shift (ECS) in dark-adapted samples demonstrate that *C. reinhardtii* CF_1F_o activity in vivo is linked to a segment in the γ-subunit redox domain. (A) Spinach CF_1F_o (PDB 6fkh) contains a salt bridge formed between γ- and β-subunit. (B) A partial alignment of the γ-subunit redox domain highlights the salt bridge-forming residue (arrowhead) that is shifted in *C. reinhardtii*. The underlined segment from *A. thaliana* replaces the native algal one in the *C. reinhardtii* γAt-loop mutant. (C) The ECS decay upon a ns flash was slowed down in γAt-loop and signals showed a long lifetime. The additional abolishment of thiol modulation re-accelerated ECS decay kinetics in γAt-loop/γC233S. (D) The ECS amplitude during a saturating light pulse was smaller in γAt-loop/γC233S, which resembled γC233S in Figure 2. Contrary, γAt-loop displayed a larger ECS amplitude during the pulse. (E) The γAt-loop ECS decay after the pulse showed a fast phase that was followed by a slow phase after ~100 ms darkness, resembling *A. thaliana* kinetics in Figure 1B. The γAt-loop/γC233S resembled γC233S in Figure 2C.

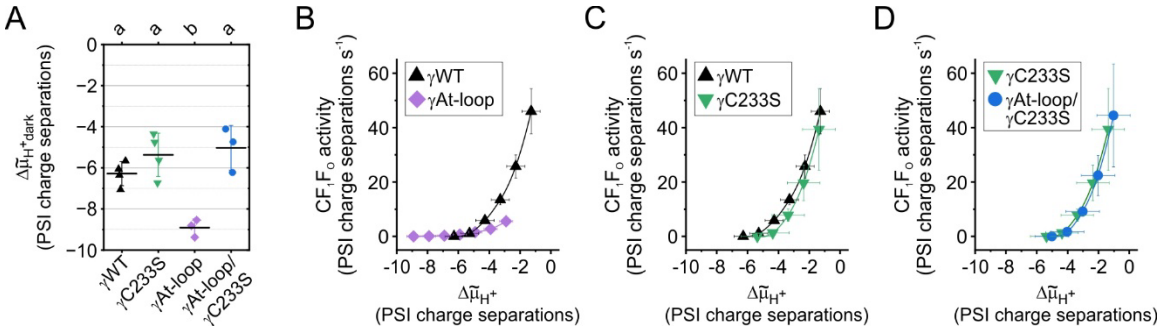

Figure 4. CF_1F_o activity profiles revealed that the hairpin segment in the γ-subunit redox domain is rate limiting in vivo in the presence of thiol modulation. (A) The $\Delta\tilde{\mu}_{H^+dark}$ equilibrated in the CF_1F_o mutants with slight variations (means of *N*=3–4 ± SD are shown, miniscules on top indicate significances using One-Way ANOVA/Fisher-LSD, *P* > 0.05). (B) A progressive increase in wild type CF_1F_o activity was observed the more the membrane was disequilibrated, starting from 0 at equilibrium on the very left to ~45 PSI charge separations s^{-1} at about ~1 unit below the maximal $\Delta\tilde{\mu}_{H^+}$ reference that was set to 0. The activation threshold was elevated in γAt-loop since CF_1F_o activity was picking up ~6 PSI charge separations s^{-1} at a $\Delta\tilde{\mu}_{H^+}$ of -2.9 units. At this level the wild type was ~3-fold as active and it started to synthesize ATP equal to ~6 PSI charge separations s^{-1} at a $\Delta\tilde{\mu}_{H^+}$ of -4.3 units. (C) No significant differences were seen in γC233S. (D) The plant-like and algal hairpin were very similar once γC233S prohibited thiol modulation.

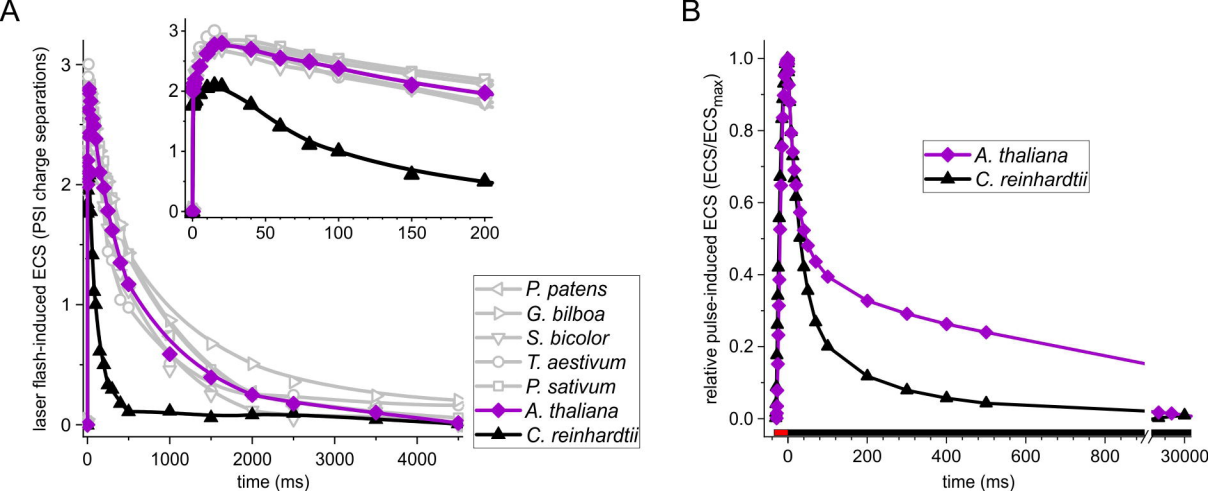
A
laser flash-induced ECS (PSI charge separations)
time (ms)
P. patens
G. bilboa
S. bicolor
T. aestivum
P. sativum
A. thaliana
C. reinhardtii
B
relative pulse-induced ECS (ECS/ECS$_{max}$)
time (ms)
A. thaliana
C. reinhardtii

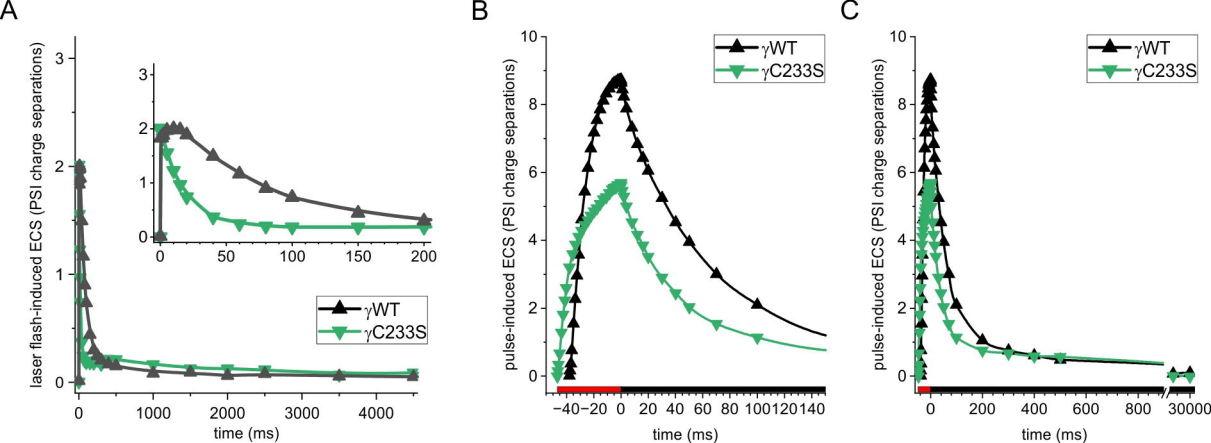
A
laser flash-induced ECS (PSI charge separations)
time (ms)
γWT
γC233S
B
pulse-induced ECS (PSI charge separations)
time (ms)
γWT
γC233S
C
pulse-induced ECS (PSI charge separations)
time (ms)
γWT
γC233S

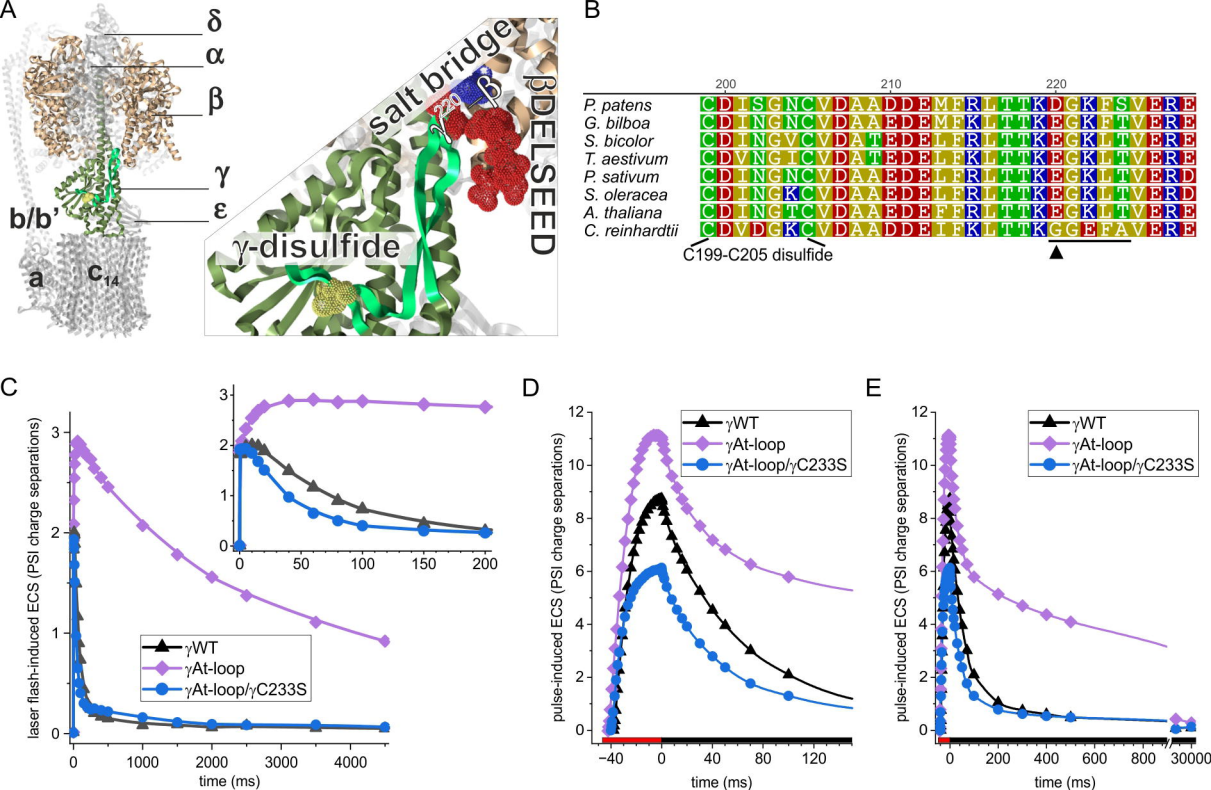
A
δ
α
β
γ
ε
b/b'
a
c14
salt bridge
γ-disulfide
βDELSEED
B
200
210
220
P. patens
G. bilboa
S. bicolor
T. aestivum
P. sativum
S. oleracea
A. thaliana
C. reinhardtii
C199-C205 disulfide
C
laser flash-induced ECS (PSI charge separations)
time (ms)
γWT
γAt-loop
γAt-loop/γC233S
D
pulse-induced ECS (PSI charge separations)
time (ms)
γWT
γAt-loop
γAt-loop/γC233S
E
pulse-induced ECS (PSI charge separations)
time (ms)
γWT
γAt-loop
γAt-loop/γC233S

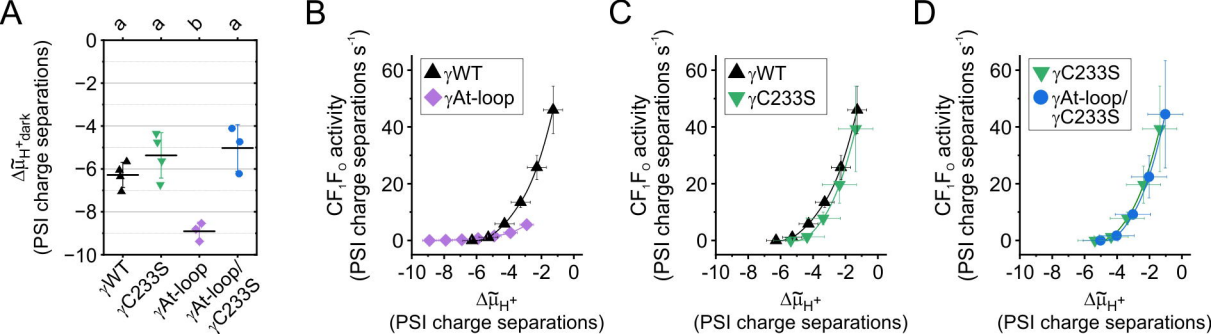
A
a
a
b
a
0
−2
−4
−6
−8
−10
$\Delta\tilde{\mu}_{H^+dark}$
(PSI charge separations)
γWT
γC233S
γAt-loop
γAt-loop/
γC233S
B
γWT
γAt-loop
CF_1F_o activity
(PSI charge separations s^{-1})
60
40
20
0
-10 -8 -6 -4 -2 0
$\Delta\tilde{\mu}_{H^+}$
(PSI charge separations)
C
γWT
γC233S
CF_1F_o activity
(PSI charge separations s^{-1})
60
40
20
0
-10 -8 -6 -4 -2 0
$\Delta\tilde{\mu}_{H^+}$
(PSI charge separations)
D
γC233S
γAt-loop/
γC233S
CF_1F_o activity
(PSI charge separations s^{-1})
60
40
20
0
-10 -8 -6 -4 -2 0
$\Delta\tilde{\mu}_{H^+}$
(PSI charge separations)